

Facile fabrication of yolk-shell structured porous Si-C microspheres as effective anode materials for Li-ion batteries

*Yachao Ru, David G. Evans, Hong Zhu and Wensheng Yang**

State Key Laboratory of Chemical Resource Engineering, Beijing University of Chemical Technology, Beijing 100029, China

*Email: yangws@mail.buct.edu.cn

Supporting materials include:

Part I. Experimental details

Preparation

Characterization

Part II. Supplementary figures

Part I. Experimental details

Preparation

Preparation of SiO₂@Void@mpC

For a typical synthesis of SiO₂@void@mpC, 400 mg of the monodisperse silica spheres (~1200 nm, purchased from Unisize Technology (Changzhou) Co., Ltd.), 200 mg of triblock copolymer PEO–PPO–PEO (P123) and 120 mg of 2-amino-2-hydroxymethyl-propane-1,3-diol (Tris) were dissolved and dispersed in 100 mL of deionized water. Then 400 mg of dopamine hydrochloride was added to the dispersion which was stirred at room temperature for 24 h. The resulting SiO₂@polydopamine particles were collected by centrifugation and washed three times using deionized water. To obtain the SiO₂@mpC, the dried powders were placed in a tube furnace and heated under N₂ atmosphere at 400 °C for 2 h with a heating rate of 1 °C/min, and then at 800 °C for 3 h with a heating rate of 5 °C/min. Finally, to get the SiO₂@void@mpC, the SiO₂@mpC powders were immersed in 2 M NaOH aqueous solution and etched for 20 min at 70 °C, followed by centrifugation and washing three times with distilled water. For the purposes of comparison, SiO₂@L_Void@mpC and porous hollow carbon spheres were obtained by extending the immersion time in aqueous NaOH solution to 30 min and 4 h respectively.

Preparation of mpSi@Void@mpC

The as-synthesized SiO₂@void@mpC (150 mg) and magnesium powder (100 mg) were put in a corundum boat, and then heated in a tube furnace at 750 °C for 6 h under an Ar atmosphere. The heating ramp rate was kept at 5 °C/min. The resulting powder was first immersed in HCl solution (25 mL, 2 M) for 12 h, and then immersed in HF solution (25 mL, 5 wt.%) for 1 h to remove MgO, residual Mg and SiO₂. Finally the sample was washed with ethanol and distilled water by centrifugation four times and vacuum-dried at 80 °C for 12 h to afford the mpSi@Void@mpC particles. For the purposes of comparison, mpSi@L_Void@mpC and mpSi/SiC@mpC spheres were synthesized according to the same preparation procedure above for mpSi@Void@mpC by using SiO₂@L_Void@mpC and SiO₂@mpC as precursors, respectively. The synthetic mpSi/SiC@mpC spheres consist Si, C and SiC.

Preparation of mpSi and mpSi@mpC spheres for the purposes of comparison

The mpSi spheres (~500 nm, approximately the size of the inner silicon particles of mpSi@Void@mpC) were synthesized by direct magnesiothermic reduction of SiO₂ spheres (~500 nm, purchased from Unisize Technology (Changzhou) Co., Ltd.) according to the same preparation procedure for mpSi@Void@mpC. The mpSi@mpC spheres were obtained by polydopamine coating on mpSi spheres and then carbonized to get the final mpSi@mpC according to the same preparation procedure for SiO₂@mpC. The synthetic mpSi@mpC spheres consist Si and C.

Characterization

Scanning electron microscopy (SEM)

SEM was carried out using a field emission scanning electron microscope (Hitachi, S-4700) with voltage of 20 kV and current of 10 μA. SEM samples were prepared by drop-drying the samples from their aqueous suspensions onto silicon substrates.

High resolution transmission electron microscopy (TEM), energy dispersive X-ray spectroscopy (EDS) elemental analysis and selected-area electron diffraction (SAED)

TEM, EDS and SAED analysis were carried out on a JEOL JEM-2100F electron microscope with an accelerating voltage of 200 kV. TEM samples were prepared by drop-drying the samples from their diluted aqueous suspensions onto copper grids.

Raman spectroscopy

Raman spectroscopy were recorded on a LabRAM ARAMIS confocal Raman microscope equipped with a 514 nm Ar-ion laser. The powder sample was pressed onto a glass substrate for Raman measurements.

Powder X-ray diffraction (XRD)

Powder X-ray diffraction (XRD) patterns were recorded on a D/max-Ultima III diffractometer operated at 40 kV, 40 mA with Cu K_α radiation ($\lambda = 0.154$ nm).

Thermogravimetric analysis (TG)

Thermogravimetric analysis (TG) was carried out using a Henven HCT-1 thermogravimetric analyzer in the temperature range from room temperature to 900 °C. A heating rate of 10 °C/min in air and 10 mg of sample were used.

N₂ adsorption/desorption measurements

Brunauer–Emmett–Teller (BET) surface area and pore size distributions were

obtained from the N₂ adsorption/desorption isotherms recorded at 77 K (QUADRASORB SI, Quantachrome Instrument Corporation). Before measurements, the samples were degassed at 80 °C for 8 h.

Electrochemical measurements

Electrochemical measurements were carried out using CR2032 coin-type cells with lithium metal as the counter and reference electrode. The working electrode was composed of 60% active material, 25% acetylene black, and 15% polyvinylidene difluoride (PVDF) binder by weight. The above mixture was pressed onto a copper foil which served as a current collector. The electrode was dried at 100 °C in vacuum for 12 h. The cell was assembled in an argon filled glove box with an electrolyte of 1 M LiPF₆ in ethylene carbonate–ethyl methyl carbonate–dimethyl carbonate (EC–EMC–DMC) (1:1:1 volume ratio) solution and a separator of Celgard 2400. Galvanostatic discharge/charge measurements were performed in the potential range 0.01–1.5 V vs. Li⁺/Li using a LAND-CT2001A test system (Wuhan, China) at room temperature. Cyclic voltammetry (CV) was measured from 3 V to 0.01 V vs. Li⁺/Li at a scan rate of 0.1 mV/s using a CHI650D (Chenhua, Shanghai) electrochemical workstation. The specific capacity and current density were calculated based on the whole composite material. To record post-electrochemical testing TEM images, the electrode after electrochemical cycling was carefully disassembled and washed by ethylene carbonate in an argon filled glove box, and dried at 100 °C in a vacuum oven.

Part II. Supplementary figures

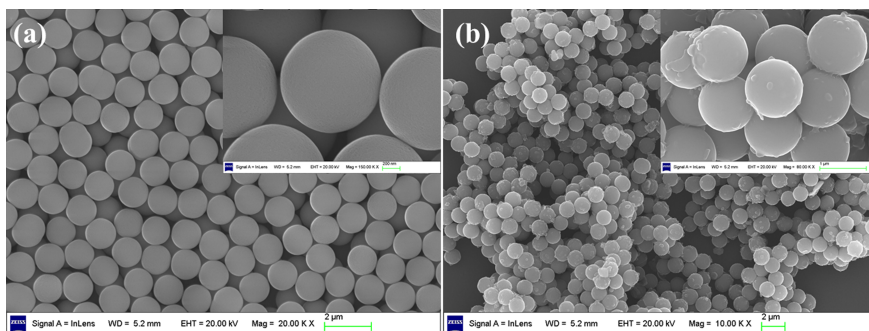


Figure S1 SEM images of SiO₂ spheres (a) and SiO₂@mpC spheres (b).

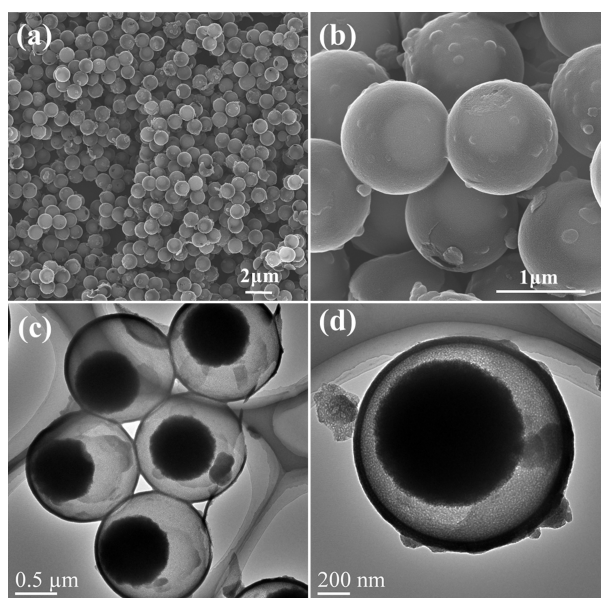


Figure S2 SEM images (a), (b) and TEM images (c), (d) of SiO₂@Void@mpC at different magnifications.

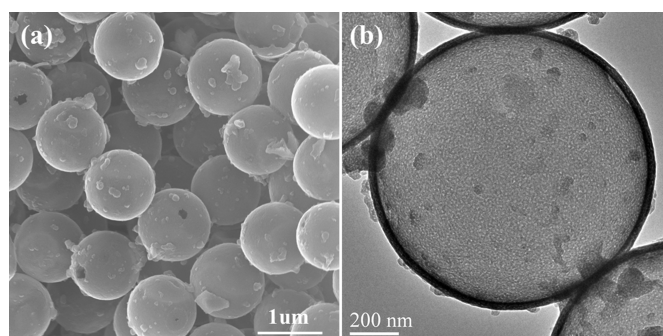


Figure S3 SEM image (a) and TEM image (b) of the porous hollow carbon spheres prepared by complete NaOH etching of SiO₂@mpC spheres.

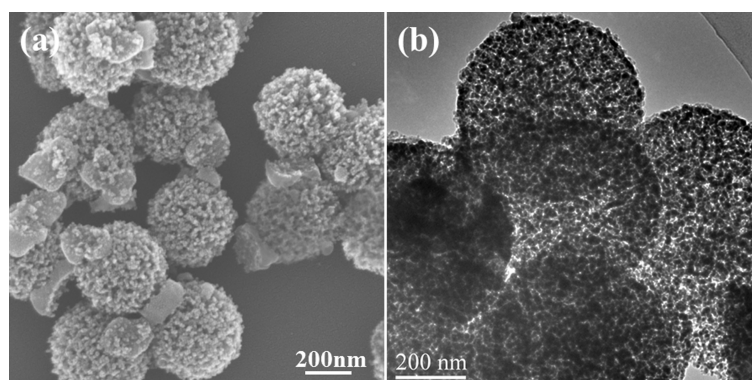


Figure S4 SEM image (a) and TEM image (b) of the mpSi spheres prepared by magnesiothermic reduction of SiO₂ spheres

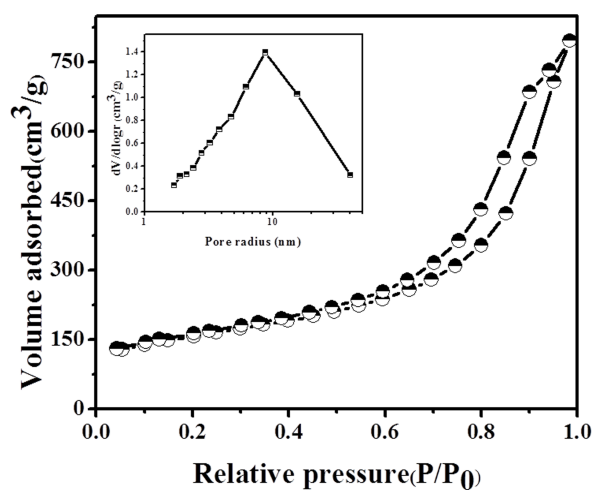


Figure S5 Nitrogen adsorption–desorption isotherms of the porous hollow carbon spheres. The inset shows the corresponding pore size distribution.

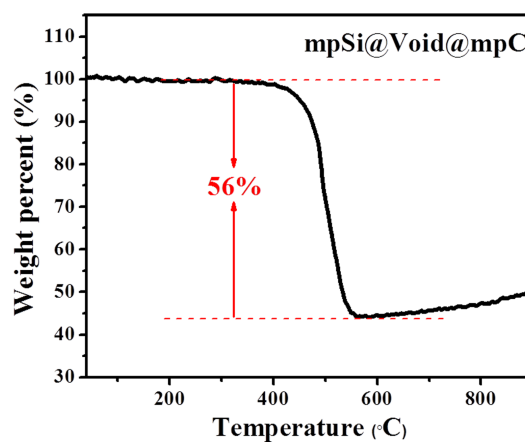


Figure S6 TG curve of mpSi@Void@mpC in air.

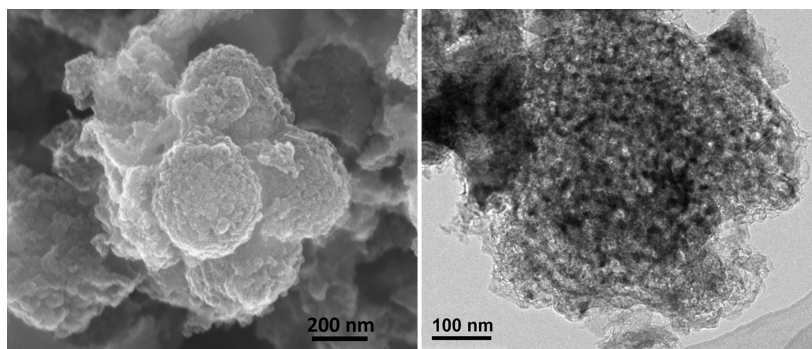


Figure S7 SEM image (a) and TEM image (b) of mpSi@mpC spheres prepared by first magnesiothermic reduction of SiO₂ to mpSi spheres and then followed by carbon coating on mpSi spheres.

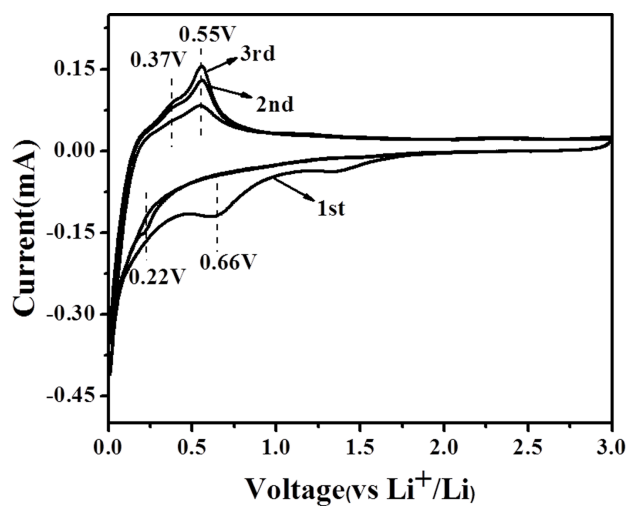


Figure S8 Cyclic voltammetry of mpSi@Void@mpC from 3 V to 0.01 V vs. Li⁺/Li at a scan rate of 0.1 mV/s.

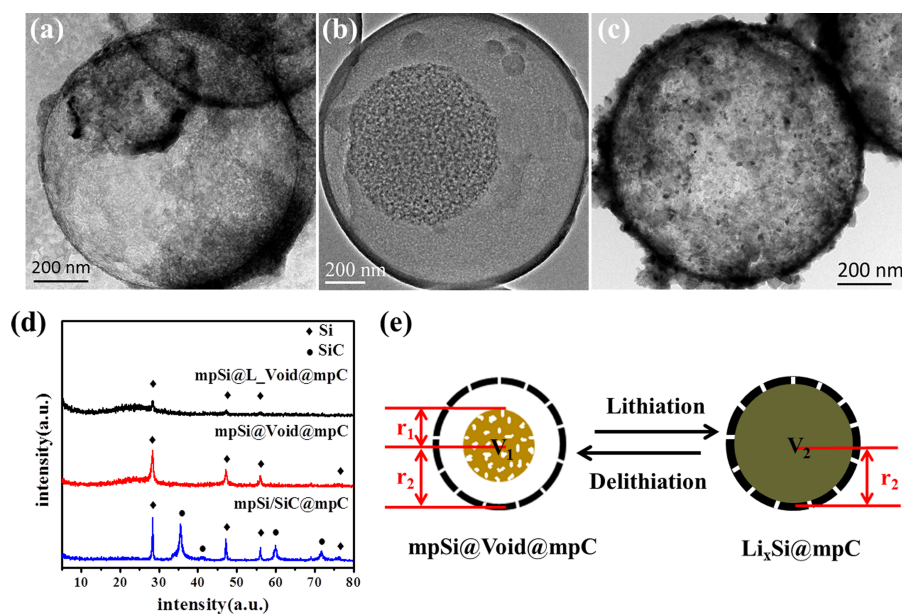


Figure S9 TEM images of mpSi@L_Void@mpC (a), mpSi@Void@mpC (b) and mpSi/SiC@mpC (c); XRD patterns (d) of mpSi@L_Void@mpC, mpSi@Void@mpC and mpSi/SiC@mpC; Schematic figure (e) showing the yolk-shell structured porous Si-C nanoparticles before and after lithiation process.

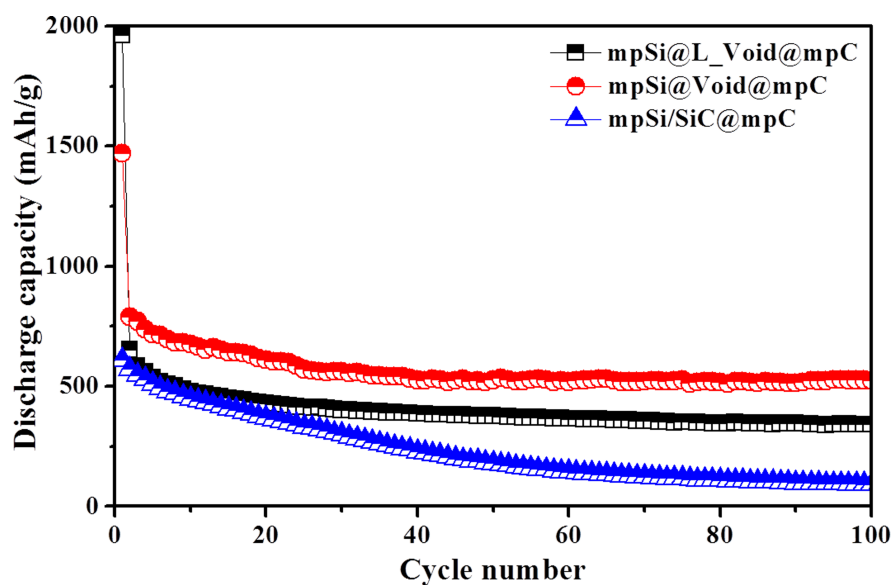


Figure S10 Cycling stabilities of mpSi@L_Void@mpC, mpSi@Void@mpC and mpSi/SiC@mpC.